J Intell Robot Syst (2014) 73:137–155
DOI 10.1007/s10846-013-9913-8

Chattering-Free Sliding Mode Altitude Control for a Quad-Rotor Aircraft: Real-Time Application

Iván González · Sergio Salazar · Rogelio Lozano

Received: 1 September 2013 / Accepted: 12 September 2013 / Published online: 4 October 2013

Abstract Nowadays, the chattering problem in sliding mode control is one of the most important points to consider in real-time applications. To address this problem, a real-time robust altitude control scheme is proposed for the efficient performance of a Quad-rotor aircraft system using a continuous sliding mode control. The sensing of altitude measurement sensing is performed by a pressure sensor in order to obtain a robust altitude control of the vehicle in hovering mode both indoor and outdoor. The altitude measurement has the advantage of introducing this state information directly in the closed loop control which should be very useful for achieving robust stabilization of the altitude control. Accordingly, we propose a sliding mode control strategy without chattering. The sliding mode control proposed removes the chattering phenomenon by replacing a sign function with a high-slope saturation function. The control algorithm is derived from the Lyapunov stability theorem. Moreover, we have assumed that the actuators are able to respond quickly and accurately and we have not enforced limits on the control signals for a real-time application. Finally, to verify the satisfactory performance of proposed nonlinear control law, several simulations and experimental results of the Chattering-free sliding mode control for the Quad-rotor aircraft in the presence of bounded disturbances are presented.

Keywords Sliding mode control · Chattering reduction · Quad-rotor aircraft · Embedded control system

This work was supported by CONACyT, UMI-LAFMIA 3175 CNRS and CINVESTAV-IPN.

I. González (✉)
Department of Automatic Control and UMI LAFMIA 3175 CNRS at CINVESTAV-IPN,
Av. IPN 2508 San Pedro Zacatenco,
07360 México D.F., México
e-mail: igonzalez@ctrl.cinvestav.mx

S. Salazar · R. Lozano
UMI LAFMIA, CINVESTAV-IPN, Av. IPN 2508
San Pedro Zacatenco, 07360 México D.F., México

S. Salazar
e-mail: ssalazar@ctrl.cinvestav.mx

R. Lozano
e-mail: rlozano@hds.utc.fr

R. Lozano
UTC-HEUDIASyC, Centre de Recherches de
Royallieu, 60205, Compiegne, France

1 Introduction

Unmanned Aerial Vehicles (UAV) are an important research topic in recent decades due to the wide range of applications in particular

Quad-rotor aircraft systems [5]. The control of a UAV aircraft involve research in various areas such as digital filtering, estimation of the position based on GPS, data fusion of sensors and so on. Now, is well known that, not exist in the real world, an ideal or perfect system that is not subject to certain disturbances or uncertainties in performance for which it was designed. That is why, in recent decades several researchers worldwide have focused on developing and establishing Robust control laws [6, 12, 13] to mention a few, in order to attenuate, compensate or control these disturbances for a certain range to achieve acceptable performance for the systems. Altitude and attitude control in a Quad-rotor aircraft involves research in various areas such as Mechatronics, Control theory and so on.

In [4] the author has proposed a method to improve the altitude control of the Quad-rotor aircraft, using sliding mode control for both translational and rotational dynamics of the Quad-rotor aircraft. This approach is based on implementing a smoothed *sign* function utilizing the approximation $sign\,(s) \approx \frac{s}{|s|+\varepsilon}$ where $\varepsilon > 0$. Since the sliding mode entails $s \approx 0$, the noise in the observed quantities becomes highly effective and the controller can generate unnecessarily large control signals. This is known as the chattering in the related literature, [11]. Otherwise, in [8] authors propose a novel sliding mode control without chattering. The proposed sliding mode control removes the undesired chattering phenomenon significantly by replacing a sign function with a continuous function.

This paper presents the real-time implementation of [4] and [8] to obtain a robust controller of the altitude of our Quad-rotor aircraft for a given reference. The advantage of using chattering-free sliding mode control is that it is possible to eliminate disturbances unwanted such as small wind gusts or disturbances which may exist even in measurements of the pressure sensor. The vehicle built to test this control strategy is shown in Fig. 1. The control algorithm used in this contribution is a *chattering-free sliding mode control* which is implemented on a embedded control system based on RabbitCore RCM4300 microcontroller. The performance of the overall system is evaluated in real-time experiments.

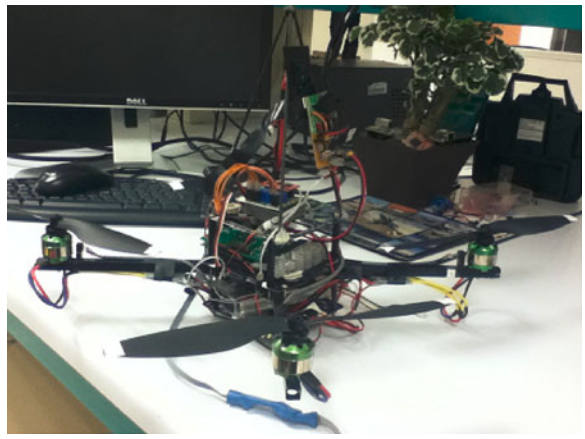

Fig. 1 Quad-rotor aircraft with the embedded electronic and sensors

This article is organized as follows: Section 2 presents the dynamical model of the Quad-rotor aircraft based on Euler-Lagrange approach. The robust altitude control based on Chattering-free sliding mode technique is described in Section 3. The architecture and operation of the prototype are described in Section 4. The effectiveness of the sliding mode control proposed without chattering phenomenon for altitude control is demonstrated through several simulations in Section 5, and verified on real-time experiments in Section 6. Finally, we present some conclusions about our work, in the Section 7.

2 Dynamical Model

Quad-Rotor Flying robot is controlled by varying the angular speed of each motor. It has four rotors arranged in a cross shape. The front and back rotors are rotating counter-clockwise and the left and right rotors are rotating clockwise. This rotor configuration produces a counter-rotating effect canceling the rotating force produced on the aerial vehicle, while conventional helicopters use the tail rotor to counter such movements. The flight direction control of the Quad-rotor is described below.

Gyroscopic effects and aerodynamic torques tend to cancel in trimmed flight. The main thrust is the sum of the thrusts of each motor, the pitch torque is a function of the difference $f_1 - f_3$, the roll torque is produced by the difference $f_2 - f_4$, and the yaw torque is the sum of $\tau_{M_1} + \tau_{M_2} + \tau_{M_3} + \tau_{M_4}$ (see Fig. 2), where τ_{M_i} is the reaction torque of motor i due to shaft acceleration and the blade drag. Let $\mathcal{I} = \{i_I, j_I, k_I\}$ be the inertial frame, $\mathcal{B} = \{i_B, j_B, k_B\}$ denote a set of coordinates fixed to the rigid aircraft as is shown in Fig. 2. Let $q = (x, y, z, \phi, \theta, \psi)^T \in \mathbb{R}^6 = (\xi, \eta)^T$ be the generalized coordinates vector which describe the position and orientation of the flying machine, so the model could be separated in two coordinate subsystems: translational and rotational. They are defined respectively by

- $\xi = (x, y, z)^T \in \mathbb{R}^3$: denotes the position of the vehicle's mass center relative to the inertial frame $\mathcal{I}$.
- $\eta = (\phi, \theta, \psi)^T \in \mathbb{R}^3$: describe the orientation of the aerial vehicle, i.e. roll, pitch and yaw angles respectively.

The dynamic model is obtained using the Euler-Lagrange approach. We can decompose the equations into translational and rotational displacement. As first step, we obtain the Lagrangian of the aerial vehicle, which is given by

$$L(q, \dot{q}) = (T_{trasl} + T_{rot}) - U \tag{1}$$

- T_{trasl} is the translational kinetic energy of the quad-rotor.

$$T_{trasl} = \frac{1}{2} m \dot{\xi}^T \dot{\xi} \tag{2}$$

- T_{rot} is the rotational kinetic energy of the quad-rotor.

$$T_{rot} = \frac{1}{2} \dot{\eta}^T \mathbb{J} \dot{\eta} \tag{3}$$

- U is the potential energy of the quad-rotor.

$$U = mgz \tag{4}$$

The model of the full Quad-rotor aircraft dynamics is obtained from the Euler-Lagrange equations with external generalized force $F_{\mathcal{B}}$ and generalized moment τ_η where $F_{\mathcal{I}}$ is the translational force applied to the Quad-rotor aircraft due to the control input. Then

$$F_{\mathcal{B}} = (0, 0, u)^T \tag{5}$$

where u is the sum of mechanical thrust forces: $u = f_1 + f_2 + f_3 + f_4$ with $f_i = k_i \omega_i^2$ for $i = 1, 2, 3, 4$, $k_i > 0$ is a constant and ω_i is the angular speed of motor i, as shown in Fig. 2. This force vector can be expressed in the inertial frame as

$$F_{\mathcal{I}} = R^{\mathcal{B}\to\mathcal{I}} F_{\mathcal{B}} \tag{6}$$

where $R^{\mathcal{B}\to\mathcal{I}}$ is the rotation matrix which is defined by

$$R^{\mathcal{B}\to\mathcal{I}} = \begin{pmatrix} c_\theta c_\psi & s_\psi c_\theta & -s_\theta \\ c_\psi s_\theta s_\phi - s_\psi c_\phi & s_\psi s_\theta s_\phi + c_\psi c_\phi & c_\theta s_\phi \\ c_\psi s_\theta s_\phi + s_\psi c_\phi & s_\psi s_\theta s_\phi - c_\psi c_\phi & c_\theta c_\phi \end{pmatrix} \tag{7}$$

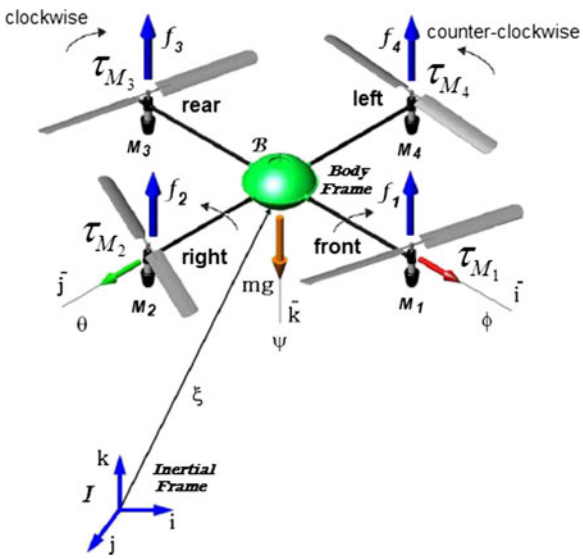

Fig. 2 *Inertial* and *Body* frames of the mini-UAV Quad-rotor

The generalized moments on the η variables are denoted by $\tau_\eta = \left(\tau_\phi \ \tau_\theta \ \tau_\psi\right)^T$ where

$$\tau_\phi = (f_3 - f_1)\, l$$
$$\tau_\theta = (f_2 - f_4)\, l$$
$$\tau_\psi = ((f_1 + f_2) - (f_3 + f_4))\, d \tag{8}$$

where l is the distance to the center of gravity and d is the drag coefficient produced by coordinated reactive torque involving the four rotors because of the geometry of the Quad-rotor aircraft. Since the lagrangian contains no cross terms in the kinetic energy, combining $\dot{\xi}$ and $\dot{\eta}$ vectors in the Euler-Lagrange equation can be partitioned into the dynamics for the ξ coordinates and the η dynamics. So, we obtain

$$F_{\mathcal{I}} = m\ddot{\xi} + mg$$
$$\tau_\eta = J\ddot{\eta} + \dot{J}\dot{\eta} - \frac{1}{2}\frac{\partial}{\partial \eta}\left(\dot{\eta}^T J \dot{\eta}\right) \tag{9}$$

Defining the Coriolis terms and gyroscopic and centrifugal terms as

$$C(\eta, \dot{\eta})\,\dot{\eta} \ = \ \dot{J}\dot{\eta} - \frac{1}{2}\frac{\partial}{\partial \eta}\left(\dot{\eta}^T J \dot{\eta}\right) \tag{10}$$

Finally, the dynamic model of the Quad-rotor aircraft [9], is given by

$$\begin{pmatrix} m\ddot{x} \\ m\ddot{y} \\ m\ddot{z} \end{pmatrix} = \begin{pmatrix} -u\, sin\,\theta \\ u\, sin\,\phi\, \cos\,\theta \\ u\, \cos\,\phi\, \cos\,\theta \end{pmatrix} + \begin{pmatrix} 0 \\ 0 \\ -mg \end{pmatrix} \tag{11}$$

$$\mathbb{J}\ddot{\eta} \ = \ \tau_\eta - C(\eta, \dot{\eta})\dot{\eta} \tag{12}$$

where x and y are the coordinates in the horizontal plane and z is the vertical position, whereas that ϕ is the roll angle around the x-axis, θ is the pitch angle around the y-axis and ψ is the yaw angle around the z-axis for the vector $\eta = (\phi, \theta, \psi)^T$.

3 Nonlinear Control Law Strategy

In this section we present a control law for the altitude control of the Quad-rotor aircraft based on sliding-mode technique. The goal of control is the stabilization in altitude at a given reference along some flight mission. Such that the coordinated control of all four rotors will provide the desired altitude control.

3.1 Altitude Robust Control with Sliding Mode Control

Since altitude control concerns only the displacement in the z-axis, one can consider the following reduced model described in Eq. 11, where

$$\ddot{z} \ = \ \frac{1}{m}(u \ \cos\,\phi\, \cos\,\theta - mg\,) \tag{13}$$

Now, the design problem is to enforce the behavior of the system states towards the desired trajectories, which are known. Denote the reference trajectories by $\dot{z}_d$ and z_d which is velocity and altitude desired respectively. Afterwards, we define the tracking errors by $e_z = z - z_d$ and $\dot{e}_z = \dot{z} - \dot{z}_d$, where z_d is the desired altitude.

First of all, the Sliding Mode control scheme introduces a "*sliding surface*" along which the sliding motion is to take place. This surface is denoted by s and is defined as follow

$$s = \left(\frac{d}{dt} + \lambda\right) e_z$$
$$s = \dot{e}_z + \lambda e_z \tag{14}$$

where $\lambda > 0$ is the slope of the sliding line. If a control law enforces the trajectories in the phase space such that $s = 0$ in Eq. 14, then the errors converge asymptotically to origin due to

$$0 = \dot{e}_z + \lambda e_z$$
$$\dot{e}_z = -\lambda e_z \tag{15}$$

for which it is known that its solution is: $e_z(t) = e_z(0)\, e^{-\lambda t}$. In order to provide global asymptotic stability about the equilibrium point, we propose the following Lyapunov function candidate given as

$$V = \frac{1}{2}s^2 \tag{16}$$

The time derivative of the Lyapunov function candidate in Eq. 16 can be computed as follows

$$\dot{V} = s\dot{s} \tag{17}$$

then, doing the mathematical operations corresponding, we have that

$$\dot{V} = s\left(\ddot{e}_z + \lambda \dot{e}_z\right)$$
$$\dot{V} = s\left(\ddot{z} - \ddot{z}_d + \lambda\left(\dot{z} - \dot{z}_d\right)\right) \tag{18}$$

after, we need that $\ddot{z}_d = 0$ and $\dot{z}_d = 0$ therefore

$$\dot{V} = s\left(\ddot{z} + \lambda \dot{z}\right) \tag{19}$$

then, substituting Eq. 13 in Eq. 19 leads to

$$\dot{V} = s\left(\frac{1}{m}\left(u \ \cos\ \phi\ \cos\ \theta - mg\ \right) + \lambda \dot{z}\right) \tag{20}$$

Also, we can consider presence of bounded disturbances $f(z, \dot{z})$, as follows

$$\dot{V} = s\left(\frac{1}{m}\left(u \ \cos\ \phi\ \cos\ \theta - mg\ \right) + \lambda \dot{z} + f(z, \dot{z})\right) \tag{21}$$

where we have to drive the variable s in Eq. 14 to zero in finite time by means of the control u. Therefore, assuming that

$$u = \frac{m\left(-\lambda \dot{z} + mg\right)}{\cos\ \phi\ \cos\ \theta} + \nu \tag{22}$$

and substituting it into Eq. 21 we obtain

$$\dot{V} = s\left(f(z, \dot{z}) + \nu\right) = sf(z, \dot{z}) + s\nu \leq |s| L + s\nu \tag{23}$$

then

$$\dot{V} \leq |s| L + s\nu \tag{24}$$

selecting

$$\nu = -\rho\ sign(s) \tag{25}$$

where $\rho > 0$ and $sign(s) = \frac{s}{|s|}$ substituting into Eq. 24 we obtain

$$\dot{V} \leq |s| L + s\left(-\rho \frac{s}{|s|}\right) = |s| L - |s| \rho \tag{26}$$

therefore

$$\dot{V} \leq -|s|\left(\rho - L\right) \tag{27}$$

Finally, the Sliding Mode Control law u proposed below will drive the Quad-rotor aircraft to the desired altitude in a finite time.

$$u = \frac{m\left(c_1 + mg\right)}{\cos\ \phi\ \cos\ \theta} \tag{28}$$

where for simplicity the term c_1 includes the Sliding Mode action, which is described as follows:

$$c_1 = -\lambda \dot{z} - \rho\ sign(s) \tag{29}$$

From control law Eq. 28 described above, it follows that the pitch and roll angles must belong to $\phi, \theta \in \left(-\frac{\pi}{2}, \frac{\pi}{2}\right)$ in order to avoid singular positions, which represents a real situation in hover flight. Then, using Eq. 28 into Eq. 13 we get

$$\ddot{z} = -\lambda \dot{z} - \rho\ sign(s) \tag{30}$$

choosing the correct values of λ and ρ in Eq. 30 ensures a stable performance of the altitude of the Quad-rotor aircraft.

3.2 Chattering Avoidance: Attenuation and Elimination

The *chattering* problem in sliding mode control is the one of the most common handicaps for applying to real-time applications. Because of imperfections in switching devices and delays, sliding mode control suffers from chattering. The sketch of Fig. 3 shows how delays can cause chattering.

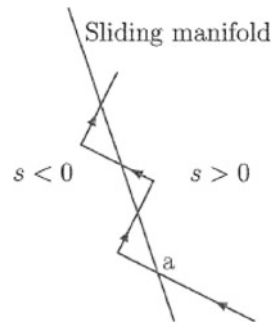

Fig. 3 *Chattering* due to delay in control switching

It depicts a trajectory in the region $s > 0$, heading toward the sliding manifold $s = 0$. It first hits the manifold at point a. In ideal sliding mode control, the trajectory should start sliding on the manifold from point a. In reality, there will be a delay between the time the sign of s changes and the time the control switches. During this delay period, the trajectory crosses the manifold into the region $s < 0$. When the control switches, the trajectory reverses its direction and heads again toward the manifold. Once again it crosses the manifold, and repetition of this process creates the "zig-zag" motion (oscillation) as shown in the sketch. Such effect is known as ***chattering***.

This phenomenon results in low control accuracy, high heat losses in electrical power circuits, and high wear of moving mechanical parts. It may also excite unmodeled high-frequency dynamics, which degrades the performance of the system and may even lead to instability. To get a better feel for chattering effect, we show several simulations the sliding mode control of the altitude equation (z-axis dynamic), in the Section 5.

In many practical control systems, including DC-motors and aircraft control, it is important to avoid control chattering [2, 3] by providing continuous/smooth control signals, for instance, aircraft aerodynamic surfaces cannot move back and for with high frequency but at the same time it is desirable to retain the robustness/insensitivity of the control system to bounded model uncertainties and external disturbances.

There are several methods to reduce the effect of the chattering in the control signal. One solution to make the control input in Eq. 28 continuous/smooth, is to approximate the discontinuous function $v = -\rho\ sign\,(s)$ by some continuous/smooth function. For instance, we will present a technique for reducing or eliminating chattering, which consists of replacing signum function "$sign\,(\cdot)$" by a high-slope saturation function "$sat\,(\cdot)$", therefore, the modified altitude control using continuous sliding mode is taken as

$$u = \frac{m\left[\left\{-\lambda\dot{z} - \rho\ sat\left(\frac{s}{\varepsilon}\right)\right\} + mg\right]}{\cos\ \phi\ \cos\ \theta} \tag{31}$$

where $sat\,(\cdot)$ is the *saturation function* defined by

$$sat\,(s) = \begin{cases} s, & if\ \ |s| \le 1 \\ \text{sgn}\,(s)\,, & if\ \ |s| > 1 \end{cases}$$

and ε is a positive constant. The signum and saturation functions are shown in Fig. 4. The slope of the linear portion of $sat\,(s/\varepsilon)$ is $1/\varepsilon$. Good approximation requires the use of small ε. In the limit, as $\varepsilon \to 0$, the saturation function $sat\,(s/\varepsilon)$ approaches the signum function $\text{sgn}\,(s)$. In [7], Chapter 14; can be found the corresponding analysis of the *continuous* sliding mode controller. Finally, a few simulations and real-time experiments were done to validate the performance of the control law proposed to reduce the chattering effect.

3.3 Yaw Control

Now, the yaw angular position $\ddot{\psi}$ can be controlled by applying

$$\tau_\psi = -a_{\psi_1}\dot{\psi} - a_{\psi_2}\,(\psi - \psi_d) \tag{32}$$

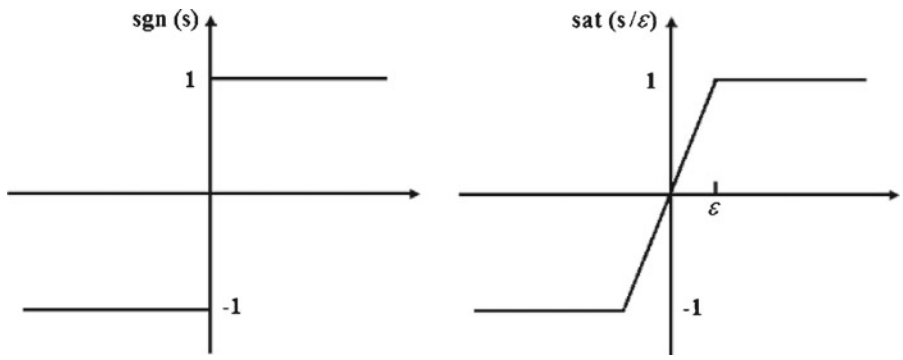

Fig. 4 The signum nonlinearity and its saturation function approximation

where ψ_d is the desired yaw angular position. Afterwards, substituting Eq. 28 into Eq. 11 and provided that $\cos\phi\cos\theta \neq 0$, we obtain

$$m\ddot{x} = -\frac{(c_1 + mg)}{\cos\ \phi}\tan\ \theta \tag{33a}$$

$$m\ddot{y} = (c_1 + mg)\tan \tag{33b}$$

$$m\ddot{z} = c_1 \tag{33c}$$

$$\ddot{\phi} = \tilde{\tau}_\phi \tag{33d}$$

$$\ddot{\theta} = \tilde{\tau}_\theta \tag{33e}$$

$$\ddot{\psi} = -a_{\psi_1}\dot{\psi} - a_{\psi_2}(\psi - \psi_d) \tag{33f}$$

By selecting the correct values for a_{ψ_1}, a_{ψ_2} ensure a fast and stable response in the yaw axis.

3.4 Roll Control

Attitude control is the most important part of our Quad-rotor aircraft system, it stabilizes the orientation of the vehicle at a desired value. If c_1 is arbitrarily small, the dynamics on x and y of Eq. 33a–33f reduces to

$$\ddot{x} = -g\frac{\tan\ \theta}{\cos\ \phi} \tag{34}$$

$$\ddot{y} = g\ \tan\ \phi \tag{35}$$

First of all, we consider the dynamics in *Roll axis* given by Eqs. 33d and 35. We will implement a non-linear controller design based on Robust Nested Saturations. This type of control allows in the limit to guarantee arbitrary bounds for ϕ, $\dot{\phi}$, y and $\dot{y}$. To further simplify the analysis, we will assume that

$$\tan\ \phi \approx \phi \quad \exists \quad |\phi| < \frac{\pi}{6}$$

which is arbitrarily small and the gravitational constant

$$g = 1\ (\textit{normalized})$$

Then, rewriting Eqs. 33d and 35 we obtain

$$\ddot{y} = \phi$$
$$\ddot{\phi} = \tilde{\tau}_\phi \tag{36}$$

and if we differentiate twice $\ddot{y} = \phi$ implies that

$$y^{(iv)} = \tilde{\tau}_\phi \tag{37}$$

which represents four integrators in cascade.

The reduced dynamical model (11) and (12) is obtained from Eq. 9. However, in the Coriolis and centrifugal forces $C(\eta, \dot{\eta})$ there exist uncertainties. Moreover, the assumption that the dynamic system works in a small linear region ($\tan\ \phi \approx \phi$) and since the terms in Eq. 30 affect directly the stability of Eq. 33a and 33b. Therefore, we have considered propose a robust control law based on [1] to ensure the stability of our system (Quad-rotor aircraft) in the presence of unmodeled dynamics in Eq. 36. For which purpose the following state space variable set is suggested

$$\dot{y}_1 = y_2 + g_1 \tag{38}$$

$$\dot{y}_2 = \phi_1 + g_2 \tag{39}$$

$$\dot{\phi}_1 = \phi_2 + g_3 \tag{40}$$

$$\dot{\phi}_2 = \tilde{\tau}_\phi + g_4 \tag{41}$$

where g_1, g_2, g_3 and g_4 are the perturbation terms could result from disturbances and uncertainties, which exist in any realistic problem, affecting the dynamic system with $\|g_i\| < d$ for $i = 1, 2, 3, 4$ where $d > 0$ and is sufficiently small. Then, we propose the following control law

$$\tilde{\tau}_\phi = -\sigma_{\phi_1}\left(k_1\phi_2 + \sigma_{\phi_2}\left(\xi_{\phi_1}\right)\right) \tag{42}$$

where $\sigma_i\,(s)$ is a saturation function is defined as

$$\sigma\,(s) = \begin{cases} M\ if & s > M \\ s\ \ if & -M \le s \le M \\ -M\ if & s < -M \end{cases} \tag{43}$$

such that $\left|\sigma_{i(s)}\right| \le M_i$ for $i = 1, 2, \ldots n$ and ξ_{ϕ_i} will be defined later to ensure global stability. Now, to demonstrate the stability of states (y_1, y_2, ϕ_1,

ϕ_2) we propose the following Lyapunov candidate function

$$V_1 = \frac{1}{2}\phi_2^2 \tag{44}$$

Differentiating Eq. 44 with respect to time, we obtain

$$\dot{V}_1 = \phi_2 \dot{\phi}_2 \tag{45}$$

using Eqs. 41 and 42 in the equation above, we have

$$\dot{V}_1 = \phi_2 \left[-\sigma_{\phi_1} \left(k_1 \phi_2 + \sigma_{\phi_2} \left(\xi_{\phi_1} \right) \right) + g_4 \right] \tag{46}$$

Note that if

$$k_1 \, |\phi_2| > M_{\phi_2} + |g_4| \quad \Rightarrow \quad \dot{V}_1 < 0$$

this means that exist for $t > T_1$ such that

$$|\phi_2| \leq \frac{M_{\phi_2} + |g_4|}{k_1} \quad \langle bounded \rangle \tag{47}$$

Now, let us define a new variable ν_1 as follows

$$\nu_1 = \phi_2 + k_1 \phi_1 \tag{48}$$

Differentiating

$$\dot{\nu}_1 = \dot{\phi}_2 + k_1 \dot{\phi}_1 \tag{49}$$

and replacing Eqs. 40 and 41 we obtain

$$\dot{\nu}_1 = -\sigma_{\phi_1} \left(k_1 \phi_2 + \sigma_{\phi_2} \left(\xi_{\phi_1} \right) \right) + g_4 + k_1 \left(\phi_2 + g_3 \right) \tag{50}$$

Let us choose

$$M_{\phi_1} \geq 2 M_{\phi_2} \tag{51}$$

From the definition of $\sigma(s)$, we can see that $|\sigma_i(s)| \leq M_i$ for $i = 1, 2 \ldots n$. This implies that in a finite time, there exist T_1 such that $|\phi_2| \leq \left(M_{\phi_2} + |g_4| \right) / k_1$ for $t \geq T_1$. Therefore, we see that $\left| k_1 \phi_2 + \sigma_{\phi_2} \left(\xi_{\phi_1} \right) \right| \leq 2 M_{\phi_2}$ for $t \geq T_1$. It then follows that for $t \geq T_1$ we can consider

$$\sigma_{\phi_1} \left(k_1 \phi_2 + \sigma_{\phi_2} \left(\xi_{\phi_1} \right) \right) = k_1 \phi_2 + \sigma_{\phi_2} \left(\xi_{\phi_1} \right) \tag{52}$$

then, substituting equality above in Eq. 50 we get

$$\dot{\nu}_1 = -\sigma_{\phi_2} \left(\xi_{\phi_1} \right) + g_4 + k_1 g_3 \tag{53}$$

Let us define

$$\xi_{\phi_1} = k_2 \nu_1 + \sigma_{\phi_3} \left(\xi_{\phi_2} \right) \tag{54}$$

Introducing above equation in Eq. 53, it follows

$$\dot{\nu}_1 = -\sigma_{\phi_2} \left(k_2 \nu_1 + \sigma_{\phi_3} \left(\xi_{\phi_2} \right) \right) + g_4 + k_1 g_3 \tag{55}$$

Let us propose the following Lyapunov candidate function to demonstrate the stability of Eq. 48

$$V_2 = \frac{1}{2}\nu_1^2 \tag{56}$$

Differentiating the equation above with respect to time

$$\dot{V}_2 = \nu_1 \dot{\nu}_1 \tag{57}$$

using Eq. 55 in the equation above, we have

$$\dot{V}_2 = \nu_1 \left[-\sigma_{\phi_2} \left(k_2 \nu_1 + \sigma_{\phi_3} \left(\xi_{\phi_2} \right) \right) + g_4 + k_1 g_3 \right] \tag{58}$$

Note that if

$$k_2 \, |\nu_1| > M_{\phi_3} + |g_4| + k_1 \, |g_3| \quad \Rightarrow \quad \dot{V}_2 < 0$$

this means that exist for $t > T_2$ such that

$$|\nu_1| \leq \frac{M_{\phi_3} + |g_4| + k_1 \, |g_3|}{k_2} \quad \langle bounded \rangle \tag{59}$$

As for the previous case, let us define ν_2 as

$$\nu_2 = \nu_1 + k_1 k_2 y_2 + k_2 \phi_1 \tag{60}$$

Differentiating

$$\dot{\nu}_2 = \dot{\nu}_1 + k_1 k_2 \dot{y}_2 + k_2 \dot{\phi}_1 \tag{61}$$

by replacing Eqs. 39, 40 and 55 we have

$$\dot{\nu}_2 = -\sigma_{\phi_2} \left(k_2 \nu_1 + \sigma_{\phi_3} \left(\xi_{\phi_2} \right) \right) + g_4 + k_1 g_3 + k_1 k_2 \left(\phi_1 + g_2 \right) k_2 \left(\phi_2 + g_3 \right) \tag{62}$$

The upper bounds are assumed to satisfy the following condition

$$M_{\phi_2} \geq 2M_{\phi_3} \tag{63}$$

This implies that exist T_2 such that $|\nu_1| \leq \left(M_{\phi_3} + |g_4| + k_1 |g_3|\right)/k_2$ for $t \geq T_2$. From Eqs. 62 and 63, we have that $\left|k_2\nu_1 + \sigma_{\phi_3}\left(\xi_{\phi_2}\right)\right| \leq 2M_{\phi_3}$ for $t \geq T_2$. It then follows that, for $t \geq T_2$

$$\sigma_{\phi_2}\left(k_2\nu_1 + \sigma_{\phi_3}\left(\xi_{\phi_2}\right)\right) = k_2\nu_1 + \sigma_{\phi_3}\left(\xi_{\phi_2}\right) \tag{64}$$

using Eqs. 48 and 64 into Eq. 62 we obtain

$$\dot{\nu}_2 = -\sigma_{\phi_3}\left(\xi_{\phi_2}\right) + g_4 + (k_1 + k_2)\, g_3 + (k_1k_2)\, g_2 \tag{65}$$

Now, let us define ξ_{ϕ_2} as

$$\xi_{\phi_2} = k_3\nu_2 + \sigma_{\phi_4}\left(\xi_{\phi_3}\right) \tag{66}$$

So, we can rewrite Eq. 65 as

$$\dot{\nu}_2 = -\sigma_{\phi_3}\left(k_3\nu_2 + \sigma_{\phi_4}\left(\xi_{\phi_3}\right)\right) + g_4 + (k_1 + k_2)\, g_3 + (k_1k_2)\, g_2 \tag{67}$$

We now propose the following Lyapunov candidate function to demonstrate the stability for Eq. 60

$$V_3 = \frac{1}{2}\nu_2^2 \tag{68}$$

Differentiating V_3 with respect to time

$$\dot{V}_3 = \nu_2\dot{\nu}_2 \tag{69}$$

by substituting Eq. 67 in the above result, we get

$$\dot{V}_3 = \nu_2\left[-\sigma_{\phi_3}\left(k_3\nu_2 + \sigma_{\phi_4}\left(\xi_{\phi_3}\right)\right) + g_4 + (k_1 + k_2) + g_3\,(k_1k_2)\, g_2\right] \tag{70}$$

Note that if

$$k_3\,|\nu_2| > M_{\phi_4} + |g_4| + (k_1 + k_2)\,|g_3| + \cdots \cdots + (k_1k_2)\,|g_2| \quad \Rightarrow \quad \dot{V}_3 < 0$$

this means that exist for $t > T_3$ such that

$$|\nu_2| \leq \frac{M_{\phi_4} + |g_4| + (k_1 + k_2)|g_3| + (k_1k_2)|g_2|}{k_3} \quad \langle bounded \rangle \tag{71}$$

Now, to the last case, we define

$$\nu_3 = \nu_2 + k_3\phi_1 + (k_1k_2k_3)\, y_1 + (k_1 + k_2)\, k_3 y_2 \tag{72}$$

and differentiating

$$\dot{\nu}_3 = \dot{\nu}_2 + k_3\dot{\phi}_1 + (k_1k_2k_3)\, \dot{y}_1 + (k_1 + k_2)\, k_3\dot{y}_2 \tag{73}$$

Finally, if we use Eqs. 38, 39, 40 and 67 into Eq. 73 we obtain

$$\begin{aligned}\dot{\nu}_3 = {} & -\sigma_{\phi_3}\left(k_3\nu_2 + \sigma_{\phi_4}\left(\xi_{\phi_3}\right)\right) + g_4 + (k_1 + k_2)\, g_3 \\ & + (k_1k_2)\, g_2 + k_3\,(\phi_2 + g_3) + k_1k_2k_3\,(y_2 + g_1) \\ & + (k_1 + k_2)\, k_3\,(\phi_1 + g_2)\end{aligned} \tag{74}$$

Last, if we chose

$$M_{\phi_3} \geq 2M_{\phi_4} \tag{75}$$

We then have that in a finite time T_3, exist Eq. 71 for $t \geq T_3$. Now, for $t \geq T_3$, $\left|k_3\nu_2 + \sigma_{\phi_4}\left(\xi_{\phi_3}\right)\right| \leq 2M_{\phi_4}$. It then follows that,

$$\sigma_{\phi_3}\left(k_3\nu_2 + \sigma_{\phi_4}\left(\xi_{\phi_3}\right)\right) = k_3\nu_2 + \sigma_{\phi_4}\left(\xi_{\phi_3}\right) \tag{76}$$

now, using Eqs. 48, 60 and 76 into Eq. 74 we have

$$\begin{aligned}\dot{\nu}_3 = {} & -\sigma_{\phi_4}\left(\xi_{\phi_3}\right) + g_4 + (k_1 + k_2 + k_3)\, g_3 \\ & + (k_1k_3 + k_2k_3 + k_1k_2)\, g_2 + (k_1k_2k_3)\, g_1\end{aligned} \tag{77}$$

We propose ξ_{ϕ_3} of the following form

$$\xi_{\phi_3} = k_4\nu_3 \tag{78}$$

then, we have

$$\begin{aligned}\dot{\nu}_3 = {} & -\sigma_{\phi_4}\,(k_4\nu_3) + g_4 + (k_1 + k_2 + k_3)\, g_3 \\ & + (k_1k_3 + k_2k_3 + k_1k_2)\, g_2 + (k_1k_2k_3)\, g_1\end{aligned} \tag{79}$$

Finally, we propose the last Lyapunov candidate function for Eq. 72

$$V_4 = \frac{1}{2}\nu_3^2 \tag{80}$$

by differentiating

$$\dot{V}_4 = \nu_3 \dot{\nu}_3 \tag{81}$$

substituting Eq. 79 into 81, we get

$$\dot{V}_4 = \nu_3 \left[-\sigma_{\phi_4}(k_4\nu_3) + g_4 + (k_1+k_2+k_3)\, g_3 + (k_1k_3 + k_2k_3 + k_1k_2)\, g_2 + (k_1k_2k_3)\, g_1\right] \tag{82}$$

then, if

$$k_4 |\nu_3| > |g_4| + (k_1+k_2+k_3)|g_3| + (k_1k_3 + k_2k_3 + \cdots\cdots + k_1k_2)|g_2| + (k_1k_2k_3)|g_1| \quad \Rightarrow \quad \dot{V}_4 < 0$$

this means that exist for $t > T_4$ such that

$$|\nu_3| \leq \frac{|g_4| + (k_1+k_2+k_3)|g_3|}{k_4} \cdots \cdots \frac{+(k_1k_3+k_2k_3+k_1k_2)|g_2| + (k_1k_2k_3)|g_1|}{k_4} \quad \langle bounded \rangle \tag{83}$$

3.5 Convergence Analysis

We show the convergence for ν_3, then if $k_i, g_i > 0$ for $i = 1, 2, 3, 4$ and $M_{\phi_4} > 0$ in (79) are selected sufficiently small, then $|\nu_3(t)| \to 0$ for $t \to \infty$. Therefore, if $k_i, g_i > 0$ and $M_{\phi_i} > 0$ for $i = 1, 2, 3, 4$ in Eqs. 42, 55, 67, 79 respectively, and are selected sufficiently small, then

$$|\nu_3(t)| \to 0 \tag{84}$$

$$|\nu_2(t)| \to 0 \tag{85}$$

$$|\nu_1(t)| \to 0 \tag{86}$$

$$|\phi_2(t)| \to 0 \tag{87}$$

Afterwards, from Eq. 48 and using Eqs. 86 and 87 implies

$$|\phi_1(t)| \to 0 \tag{88}$$

substituting Eqs. 85, 86 and 88 into Eq. 60 we obtain

$$|y_2(t)| \to 0 \tag{89}$$

and finally, using the results Eqs. 84, 85, 88 and 89 into Eq. 72 we get

$$|y_1(t)| \to 0 \tag{90}$$

At last, using Eqs. 48, 54, 60, 66, 72 and 78, we can rewrite Eq. 42 as follows

$$\begin{aligned}\tau_\phi = &-\sigma_{\phi_1}(k_1\phi_2 + \sigma_{\phi_2}(k_2(\phi_2 + k_1\phi_1) \\ &+ \sigma_{\phi_3}(k_3((\phi_2 + k_1\phi_1) + k_1k_2y_2 + k_2\phi_1) \\ &+ \sigma_{\phi_4}(k_4((\phi_2 + k_1\phi_1) + k_1k_2y_2 + k_2\phi_1) \\ &+ k_3\phi_1 + k_1k_2k_3y_1 + (k_1+k_2)\,k_3y_2))))\end{aligned} \tag{91}$$

This control law guarantees convergence to zero of ϕ_1, ϕ_2, y_1 and y_2.

3.6 Pitch Control

We will use for Pitch control the same procedure used in the previous section for Roll control. We now consider the dynamics in Pitch axis given by Eqs. 33e and 34. As before, we will use a control strategy such that after a finite time θ is small enough such that $\tan\theta \approx \theta$. Therefore, we have

$$\begin{aligned}\ddot{x} &= -\theta \\ \ddot{\theta} &= \tilde{\tau}_\theta\end{aligned} \tag{92}$$

Using the same procedure used for controlling the Roll control, we have

$$\begin{aligned}\tau_\theta = &-\sigma_{\theta_1}(k_1\theta_2 + \sigma_{\theta_2}(k_2(\theta_2 + k_1\theta_1) \\ &+ \sigma_{\theta_3}(k_3((\theta_2 + k_1\theta_1) - k_1k_2x_2 + k_2\theta_1) \\ &+ \sigma_{\theta_4}(k_4((\theta_2 + k_1\theta_1) - k_1k_2x_2 + k_2\theta_1) \\ &+ k_3\theta_1 - k_1k_2k_3x_1 - (k_1+k_2)\,k_3x_2))))\end{aligned} \tag{93}$$

This control law guarantees convergence to zero of θ_1, θ_2, x_1 and x_2.

4 Quad-Rotor Aircraft System Scheme

In this section we present the prototype of the Quad-rotor aircraft. The overall system scheme is

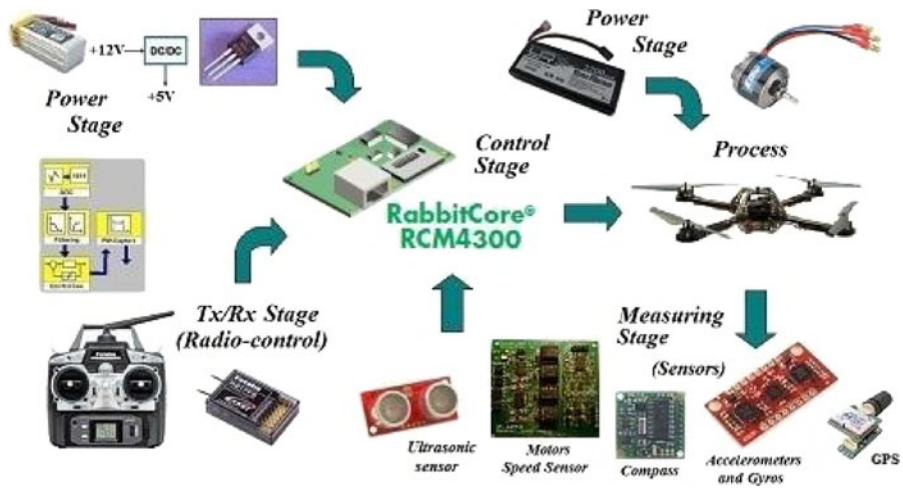

Fig. 5 Real-time embedded control architecture based on Rabbit4300 onto Quad-Rotor aircraft

shown in Fig. 5. It basically consists of four-rotors arranged in a carbon fiber frame, Measuring stage (*Sensors*), Control stage (*Embedded system: RabbitCore RCM4300*), Tx/Rx (*Radio-control*) and Power stages (*Li-Po batteries*).

4.1 Sensors Module

It consists of a home-made Inertial Measurement Unit (IMU) based on Sparkfun's Analog Combo Board Razor-6DOF Ultra-Thin (see Fig. 6). The signals from IMU are sampled using a 12-bit analog-to-digital converter. (see Fig. 6). The signals from IMU are sampled using a serial port of the microprocessor Rabbit4300. The IMU measures three angular rates $(\dot{\phi}, \dot{\theta}, \dot{\psi})$ and two angular positions (ϕ, θ) afterwards to measure the yaw angle (ψ) we use a compass CMPS03. It can produce a unique number to represent the direction the flying robot is facing. Figure 7 shows the MPX4115A series silicon pressure sensor by Motorola. It provide a high output signal and temperature compensation. The small form factor and high reliability of on-chip integration make

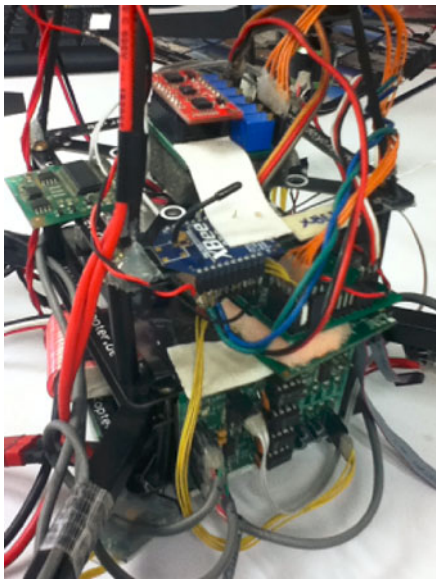

Fig. 6 Sensors arrangement to measure and altitude control of the Quad-rotor aircraft

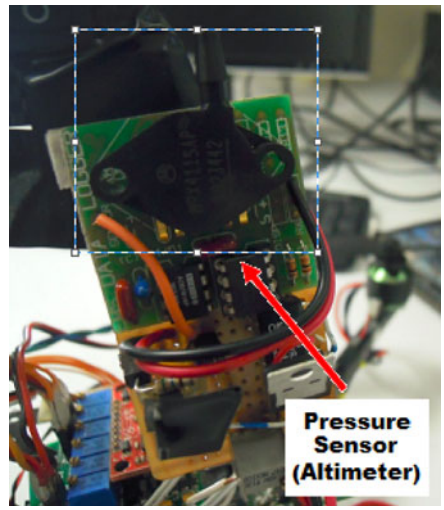

Fig. 7 MPX4115A pressure sensor used to measure the altitude of the Quad-rotor aircraft outdoor

the Motorola pressure sensor a logical and economical choice for designing our altimeter. This sensor combines advanced micromachining techniques, thin film metallization, and bipolar semiconductor processing to provide an accurate, high level analog output signal that is proportional to applied pressure. Due to the easy interface with a microcontroller is a good choice for measuring the altitude of our Quad-rotor aircraft.

4.2 Embedded Control System Based on RabbitCore RCM4300 Microcontroller

A mini RabbitCore module RCM4300 (8-Bit Flash memory program) is employed to control the attitude and altitude of our Quad-rotor aircraft system. The RCM4300 runs the control algorithm in real time to stabilize the Quad-rotor system managing the information provided by the IMU sends the control signals to the four motors. Figure 8 shows a schematic diagram of the core electronic architecture used.

The mini-core has the following main features: operates at 58.98 Mhz (10-ns Cycle Time), with 512K bits serial I2C EEPROM memory, low-power (1.8-V Core, 3.3-V I/O), 4 PWM channels (10-bit resolution), 8 ADC channels (12-bit resolution), 5 serial ports, 2 input-capture channels, 10 timers (16-bit resolution) and I^2C port.

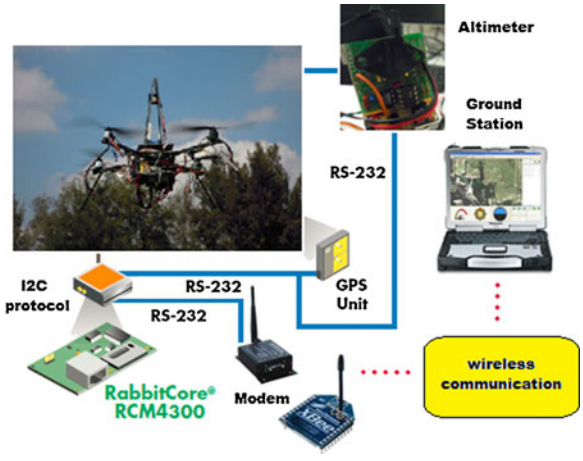

Fig. 8 Embedded control system based on Microprocessor Core module Rabbit4300

4.3 Tx/Rx and Power Stages

A commercial 7-Channel 2.4GHz radio control system (RC) from FUTABA is used to send commands reference to maneuver the Quad-rotor aircraft. The main signal is captured and decoded in such way that it allows to introduce an external input to have either manual and/or automatic operation. The radio can be used for trimming small offset deviations. In this way, the position feedback is triggered by an external RC signal from the radio. The power supply of the complete system consists of batteries (Li-Po). These kind of batteries have a wide range of power management and has the advantage that are reasonably small and light. Quad-rotor aircraft has a flight time of approximately 7 to 10 minutes with this type of Li-Po battery depending of meteorological conditions.

5 Simulation Results

Simulation results of the Quad-rotor aircraft using the sliding mode technique to the altitude control ($z - dynamic$), the chattering effect produced by sliding mode controller and the robust nested saturation control for the stabilization of the roll and pitch (ϕ, θ) angles are presented below. The control task in real-time and simulation was to compensate the initial error and stabilize the roll, pitch and yaw angles.

A short list of the parameters of the Sliding Mode control law and the Nested Saturation Control used in these simulations are briefly described in Table 1.

In the simulations, some external disturbances has been introduced to test stability robustness

Table 1 Simulations parameters for sliding mode control

Parameters	Value
Mass of the Quad-rotor aircraft, (m) [kg]	1.00
Gravitational acceleration, (g) [m/s^2]	9.81
Reaching law parameter, (ρ)	0.80
Slope parameter, (λ)	1.20

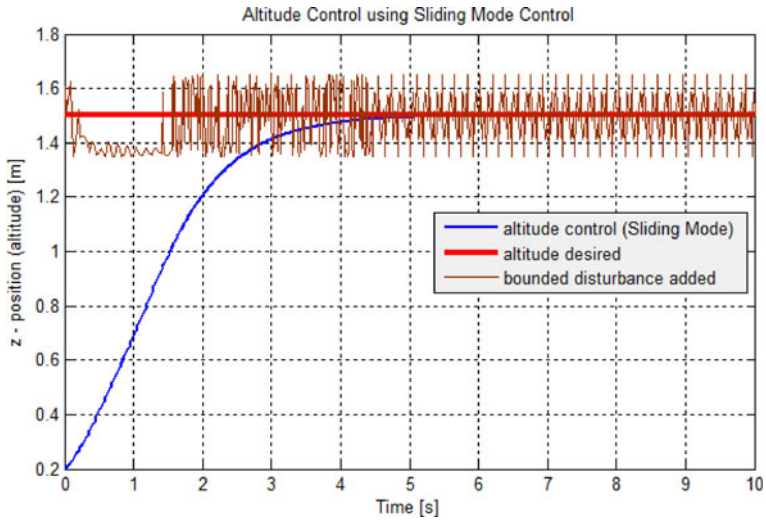

Fig. 9 *Altitude sliding mode control* behavior in the presence of bounded disturbances of the way $f(\dot{z}, z, t) = sin0.15t$. The position on the z-axis converges faster to desired altitude

in the Sliding Mode technique for the altitude control of the Quad-rotor aircraft.

5.1 Altitude Simulation Results

The simulation results of the altitude control based on sliding mode control are shown in Figs. 9, 10, 11 and 12, bounded disturbances of the way $f(\dot{z}, z, t) = sin0.15t$ were added on altitude rate value. Observer that altitude of the Quad-rotor achieved in a reasonable time to the desired altitude with *chattering phenomenon* around the altitude reference value. This statement can be observed much better in Fig. 10.

Figures 13 and 14 show simulations and performance of the modified control law in Eq. 28 when applying the saturation function as approximation of the sign function to eliminate the chattering for the altitude control in the presence of external disturbances. The reduction in the amplitude of chattering is clear. From Figs. 15 and 16, we can observer that the chattering phenomenon is significantly reduced in the control signal u applied to the actuators.

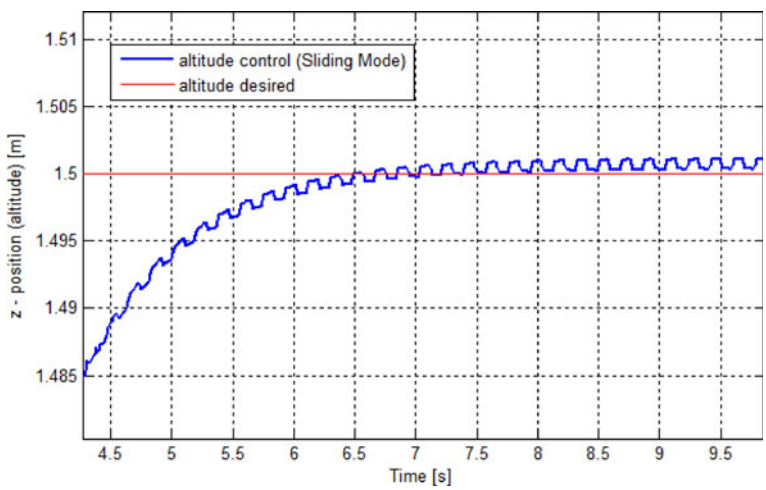

Fig. 10 Sliding mode control response on the desired altitude (*Zoom*)

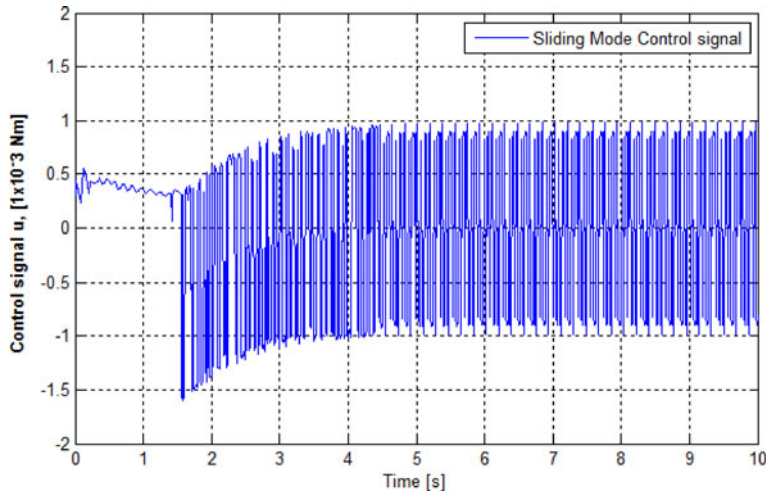

Fig. 11 Sliding mode control signal applied to the Quad-rotor aircraft to reach the desired altitude

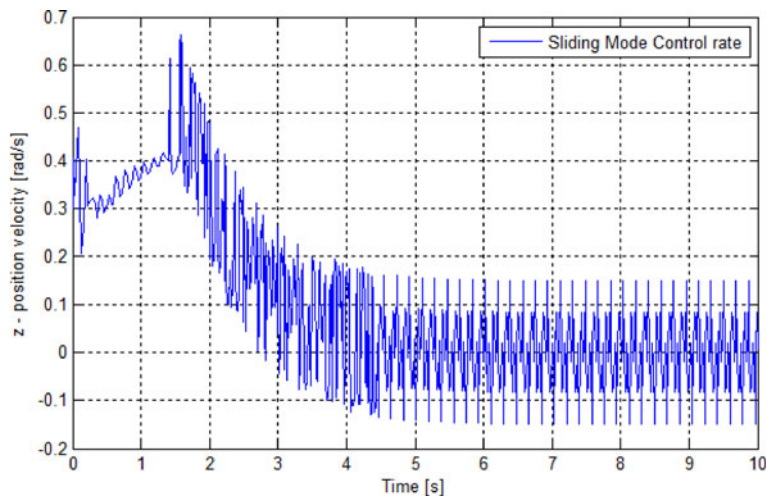

Fig. 12 *Altitude rate* behavior using Sliding Mode Control with $z(0) = 0.2$, $\dot{z}(0) = 0.3$ and bounded disturbance $f(\dot{z}, z, t) = sin0.15t$. Position on the z-axis converges faster to equilibrium

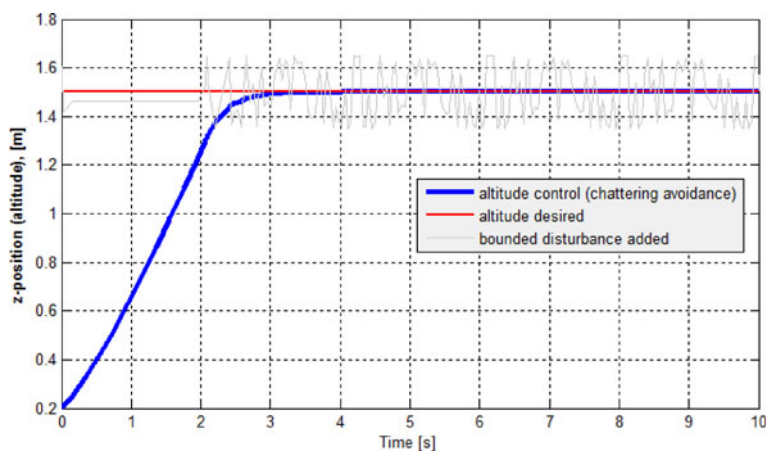

Fig. 13 Altitude control behavior using *modified sliding mode control* in the presence of bounded disturbances of the way $f(\dot{z}, z, t) = sin0.15t$. The current altitude converges faster to the desired reference (1.5 m)

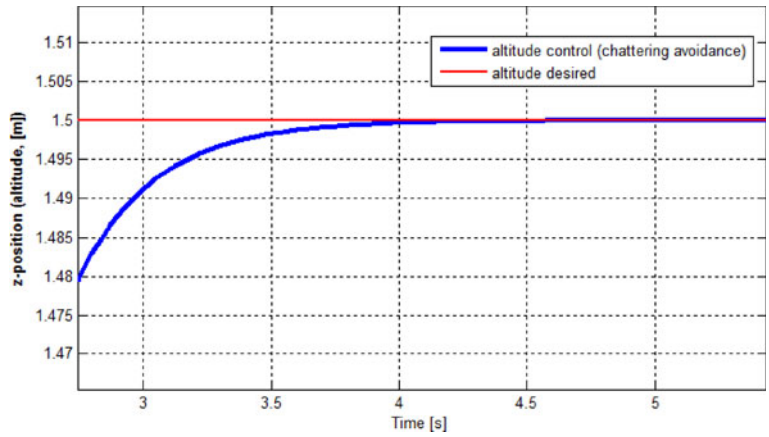

Fig. 14 Chattering-free sliding mode response on the desired altitude (*Zoom*)

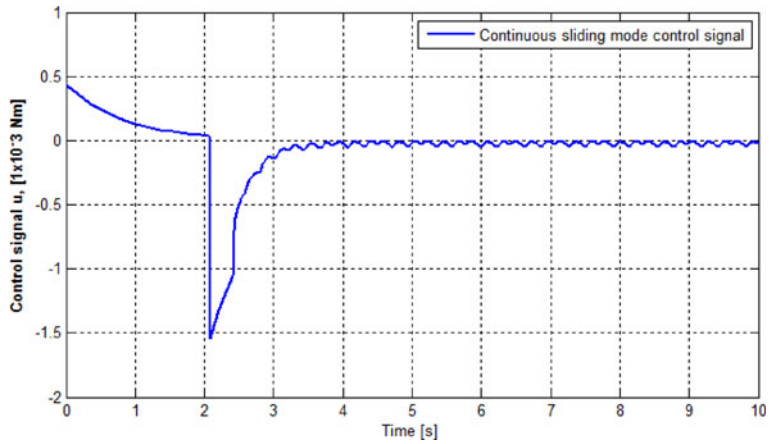

Fig. 15 *Control signal* applied to the Quad-rotor aircraft to reach the desired altitude (chattering-free approach). Observe that the amplitude of the chattering effect is significantly reduced

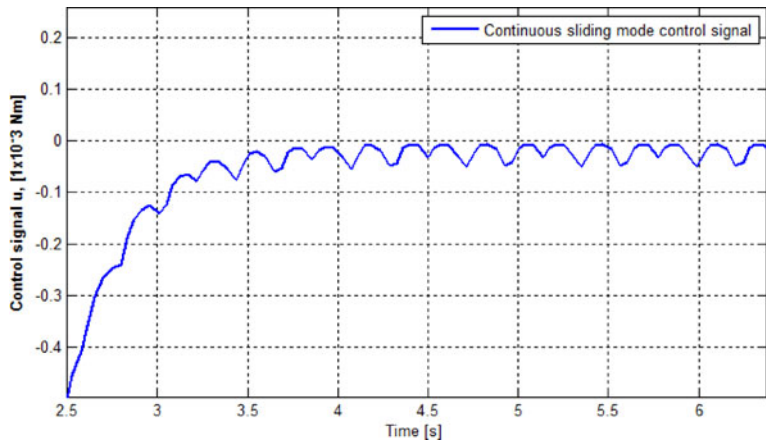

Fig. 16 *Control signal* behavior using sliding mode control with saturation function to attenuate chattering phenomenon (*Zoom*)

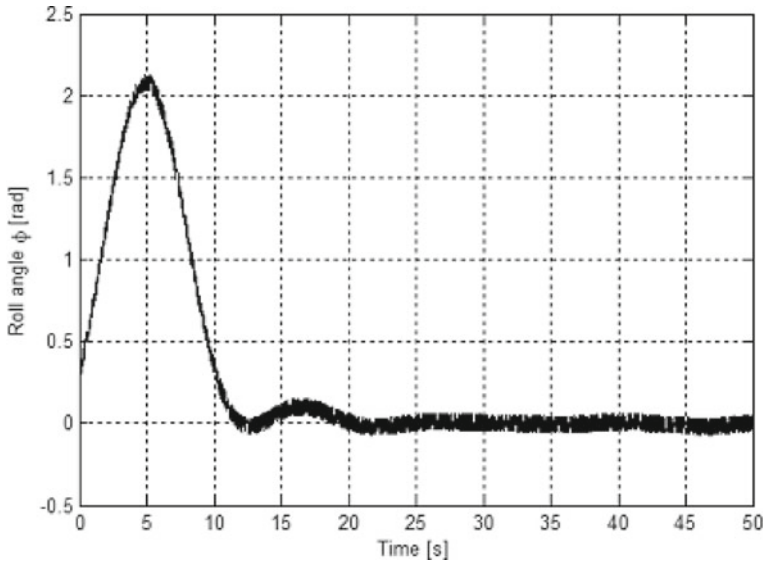

Fig. 17 Robust control law behavior of the *roll angle* with disturbances added over the whole trajectory

5.2 Attitude Simulation Results

The results of the simulation of the robust nested saturation control law for the roll and pitch (ϕ, θ) angles described in Eqs. 91 and 93 with parameters $\sigma_{\phi_1,\theta_1} = 1, \sigma_{\phi_2,\theta_2} = 0.5, \sigma_{\phi_3,\theta_3} = 0.25\ \sigma_{\phi_1,\theta_1} = 0.125$. The gains for the roll angle are $k_{\phi_1} = 0.5$, $k_{\phi_2} = 0.3$, $k_{\phi_3} = 0.2$, $k_{\phi_4} = 0.029$ and the gains for the pitch angles are $k_{\theta_1} = 0.4$, $k_{\theta_2} = 0.35$, $k_{\theta_3} = 0.25$, $k_{\theta_4} = 0.096$. The response of the system with this gains is illustrated by numerical simulations in Fig. 17 and 18. The response of the yaw angle with $\psi(0) = 0.2rad$ is presented in Fig. 19.

Clearly, the attitude angles (ϕ, θ, ψ) return in a reasonable time to the normal operation with some oscillatory behavior around the reference values and the obtained results have been found satisfactory.

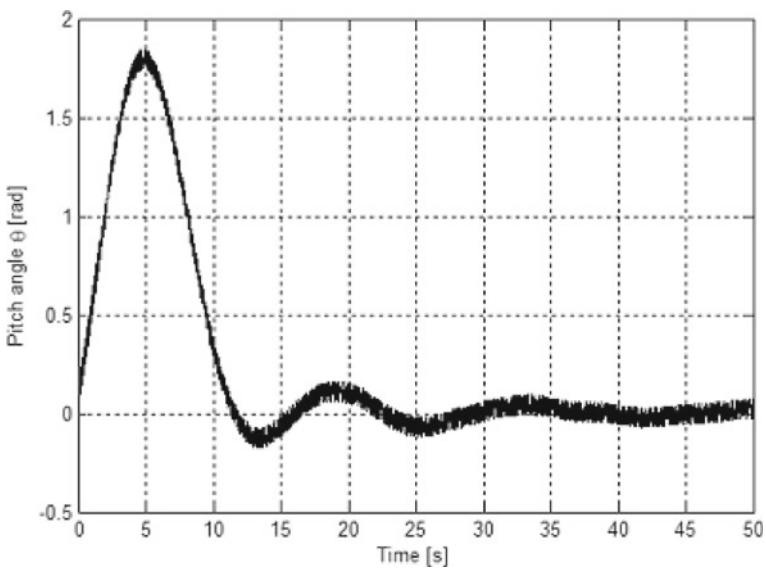

Fig. 18 Robust control law behavior of the *pitch angle* with disturbances added over the whole trajectory

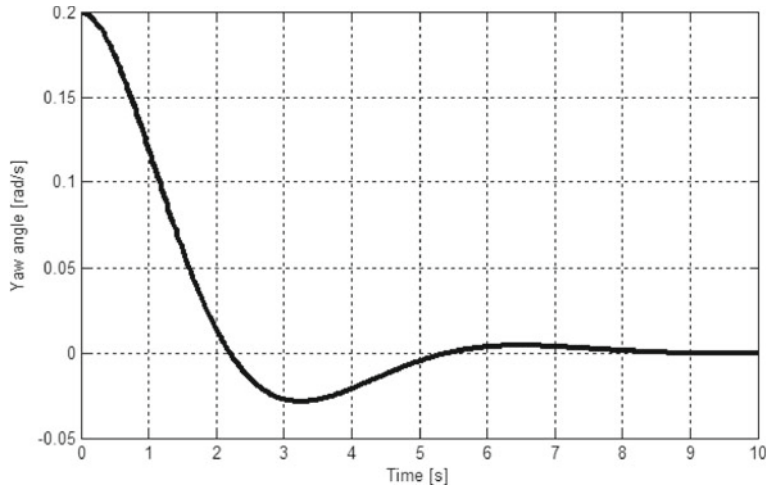

Fig. 19 Behavior of the *yaw angle* with initial conditions $\psi(0) = 0.2rad$

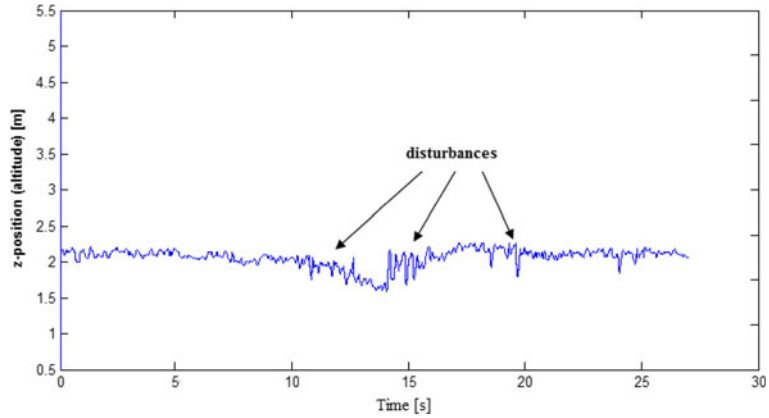

Fig. 20 *Altitude control* behavior using "continuous"sliding mode controller outdoor. The position on z-axis of the Quad-rotor aircraft converges faster to desired altitude (*horizontal plane*)

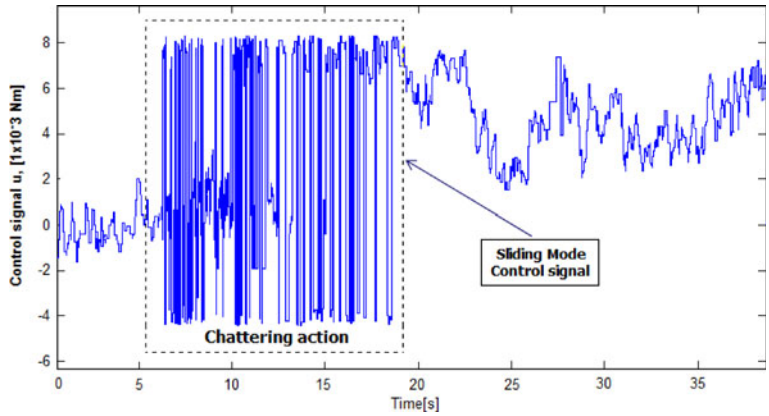

Fig. 21 *Control signal* applied to the Quad-rotor aircraft system using "continuous"sliding mode control. Notice that, the reduction in the amplitude of *chattering*

Fig. 22 Quad-rotor aircraft at hovering flight using sliding mode control without chattering phenomenon

6 Real-Time Implementation

In order to validate the altitude control using sliding mode technique without chattering phenomenon, we implemented the controller on the embedded control unit, during autonomous hover flight. We carried out several experiments to stabilize the altitude of vehicle. The controllers parameters were tuned by trial and error, until obtaining a better responses performance of the system. Figures 20, 21 and 22 present some experimental results obtained by applying the altitude control algorithm using continuous sliding mode controller.

7 Conclusions

In this paper, we present a robust altitude controller using sliding mode control without chattering. This control law consider a saturation function in order to eliminate chattering phenomenon. We developed several real-time experiments to validate the robustness algorithm proposed. In these tests we find the bounded disturbance which is used to evaluate the gains of the chattering-free sliding mode control. We consider that the control altitude is an important issue due the landing and take-off could be performed in a future work.

References

1. Arcak, M., Teel, A.R., Kokotovic, P.: Robust nested saturation redesign for systems with input unmodeled dynamics. In: Proceedings American Control Conference, pp. 150–154 (2000)
2. Bartolini, G., Ferrara, A., Usai, E.: Chattering avoidance by second-order sliding mode control. IEEE Trans. Automat. Control **43**(2), 241–246 (1998)
3. Boiko, I., Fridman, L.: Analysis of chattering in continuous sliding-mode controllers. IEEE Trans. Automat. Control **50**(9), 1442–1446 (2005)
4. Efe, M.O.: Robust low altitude behavior control of a quadrotor rotorcraft through sliding modes. In: Mediterranean Conference on Control and Automation, pp. 1–6 (2007)
5. Escareno, J., Salazar-Cruz, S., Lozano, R.: Embedded control of a four-rotor UAV. In: Proceedings American Control Conference, pp. 3936–3941 (2006)
6. Hu, Q., Fei, Q., Wu, Q., Geng, Q.: Research and application of nonlinear control techniques for Quadrotor UAV. In: 31st Chinese Control Conference, pp. 706–710 (2012)

7. Khalil, H.K.: Nonlinear Systems. Prentice Hall (2002)
8. Kim, K.J., Park, J.B., Choi, Y.H.: Chattering Free Sliding Mode Control. In: International Joint Conference SICE-ICASE, pp. 732–735 (2006)
9. Lozano, R. (ed.): Unmanned Aerial Vehicles: Embedded Control. Wiley, Hoboken, NJ (2010)
10. Salazar-Cruz, S., Escareno, J., Lara, D., Lozano, R.: Embedded control system of a four-rotor UAV. Int. J. Adapt. Control Signal Process. **21**, 189–204 (2007)
11. Slotine, J.-J.E., Li, W.: Applied Nonlinear Control. Prentice-Hall, New Jersey (1991)
12. Teel, A.R.: Global stabilization and restricted tracking for multiple integrators with bounded controls. Syst. Control Lett. **18**, 165–171 (1992)
13. Teel, A.R.: A nonlinear small gain theorem for the analysis of control systems with saturation. IEEE Trans. Automat. Control **41**(9), 1256–1271 (1996)